Nanoscience and Nanotechnology Letters
Vol. 3, 717–722, 2011

Modified Sol–Gel Synthesis to Prepare Nanocrystalline $LiCo_{1/3}Ni_{1/3}Mn_{1/3}O_2$ Cathode Suitable for Rechargeable Lithium Batteries

N. Gangulibabu, D. Bhuvaneswari, and N. Kalaiselvi*

Central Electrochemical Research Institute, Karaikudi 630006, India

Phase pure and nanocrystalline $LiCo_{1/3}Ni_{1/3}Mn_{1/3}O_2$ is synthesized at 850 °C using modified sol–gel method and the required phase purity is obtained by using a lithium and transition metal ratio of 1.1:1. A combination of citric acid as complexing agent and ammonium per sulphate as gelling catalyst results in the rapid formation of transparent gel, which upon furnace calcination yields phase pure and nanocrystalline $LiCo_{1/3}Ni_{1/3}Mn_{1/3}O_2$ powder. Powder X-ray diffraction pattern confirms the formation of phase pure $LiCo_{1/3}Ni_{1/3}Mn_{1/3}O_2$ compound and TEM images confirm the nanocrystalline nature of the title compound consisting of 50nm particle size. Cyclic voltametry and impedance spectral studies demonstrate the excellent reversibility and structural stability of $LiCo_{1/3}Ni_{1/3}Mn_{1/3}O_2$ cathode. Upon cycling, $LiCo_{1/3}Ni_{1/3}Mn_{1/3}O_2$cathode delivered a capacity as high as 162 mAh/g with a capacity retention of 99% up to 30 cycles.

Keywords: Modified Sol–Gel Method, $LiCo_{1/3}Ni_{1/3}Mn_{1/3}O_2$, Lithium Batteries, Cycling Reversibility, Specific Capacity.

1. INTRODUCTION

Rechargeable lithium batteries that have revolutionized the modern e-society have a major dependence on the electrochemical performance of cathode materials deployed in the same. Among the various cathode candidates of choice, $LiCo_{1/3}Mn_{1/3}Ni_{1/3}O_2$ possesses advantages like high specific capacity (~170 mAh/g) compared to $LiCoO_2$ (~130 mAh/g), appreciable working voltage and relatively reduced cost and toxicity due to the presence of 33% Mn, which in turn stabilizes the layered structure.

It is well known that the electrochemical performance characteristics of lithium-ion batteries could be enhanced by way of reducing the particle size of phase pure electrode materials.[1] With regard to $LiCo_{1/3}Mn_{1/3}Ni_{1/3}O_2$ cathode, cation mixing, a commonly reported problem[2] due to the closer resemblance of ionic radii of Li^+ and Ni^{2+} ions is reported to lead to phase purity related intricacies, which are detrimental to the electrochemical behaviour of the same. Hence, formation of phase pure $LiCo_{1/3}Mn_{1/3}Ni_{1/3}O_2$ compound is challenging and the preparation of nano crystalline and phase pure $LiCo_{1/3}Mn_{1/3}Ni_{1/3}O_2$ compound is still more challenging. Even though several synthesis approaches such as ceramic method,[3] acetate decomposition method,[4] hydroxide precipitation method,[5] carbonate co-precipitation method,[6] etc. are reported for the preparation of $LiNi_{1/3}Mn_{1/3}Co_{1/3}O_2$ compound, a careful selection of suitable synthesis approach alone will lead to the formation of phase pure and nano crystalline $LiCo_{1/3}Mn_{1/3}Ni_{1/3}O_2$ compound.

In this regard, modified sol–gel method that involves the uniform distribution and an atomic level mixing of reactants and gelling agent is aimed through the present study to prepare phase pure and nanocrystalline $LiCo_{1/3}Mn_{1/3}Ni_{1/3}O_2$ compound with improved lithium intercalation behaviour. Herein, the gel formed out of the homogeneous precursor solution in the formation of phase pure final product with nanocrystalline particles. Particularly, added acryl amide acts as an interlinking agent and citric acid as fuel for the formation of bond with the transition metal ions. Further, the carboxylic acid group present in citric acid (complexing agent) forms a chemical bond with the metal ions, which upon evaporation forms a viscous gel.[7] Unlike the gel formation that requires few hours in conventional approaches,[8] addition of ammonium per sulphate catalyses and aids the formation of gel well within a minute, which is the key point of currently adopted modified and rapid sol–gel method.

*Author to whom correspondence should be addressed.

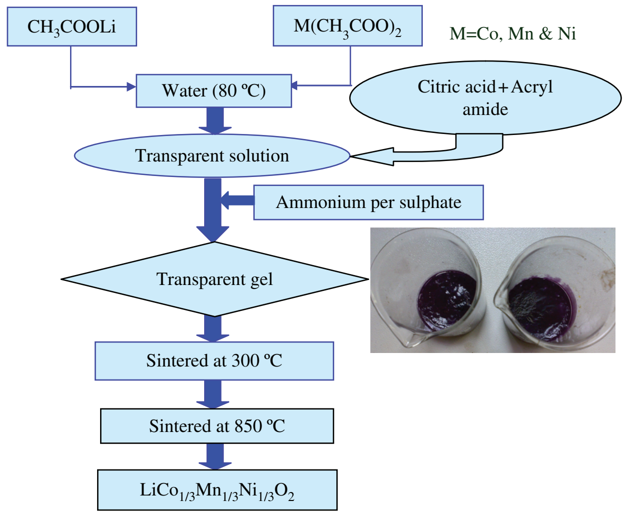

Fig. 1. Flow chart for the synthesis of $LiCo_{1/3}Mn_{1/3}Ni_{1/3}O_2$ using modified sol–gel method [formed transparent gels are seen in the beaker].

Such a modified sol–gel synthesized cathode candidate, bestowed with the formation of nanocrystalline particles is expected to exhibit enhanced battery performance, due to the much shorter diffusion distances of intercalating Li^+ ions. Accordingly, sol–gel approach adopted in the present study has resulted in the formation of phase pure $LiCo_{1/3}Ni_{1/3}Mn_{1/3}O_2$ powder with desirable physical and electrochemical characteristics, which is in accordance with the focal theme of the present work.

2. EXPERIMENTAL DETAILS

2.1. Synthesis Procedure

$LiCo_{1/3}Ni_{1/3}Mn_{1/3}O_2$material was synthesized by adopting a rapid gel forming modified sol–gel method. Herein, 3 g of citric acid and 3 g of acryl amide were added respectively as chelating and interlinking agents to the precursor solution. Subsequently, a pinch of ammonium per sulphate was added to accelerate the gel formation at about 80 °C with continuous stirring. The sequence of addition of precursor and other reagents along with the details of furnace calcination are given in Figure 1 (Flow chart).

2.2. Physical and Electrochemical Characterizations

Phase characterization was done by a powder X-ray diffraction technique on a PANalytical X'pert PRO X-ray diffractometer using Ni-filtered Cu Kα radiation (λ = 1.5406 Å) in the 2θ range 10–90° at a scan rate of 0.04°/s. Transmission electron microscopy (TEM) images were collected with a JEOL 2010F TEM operating at 200 keV and the oxidation state of individual metal atoms was confirmed from MultiLab 2000 (Thermofisher Scientific,

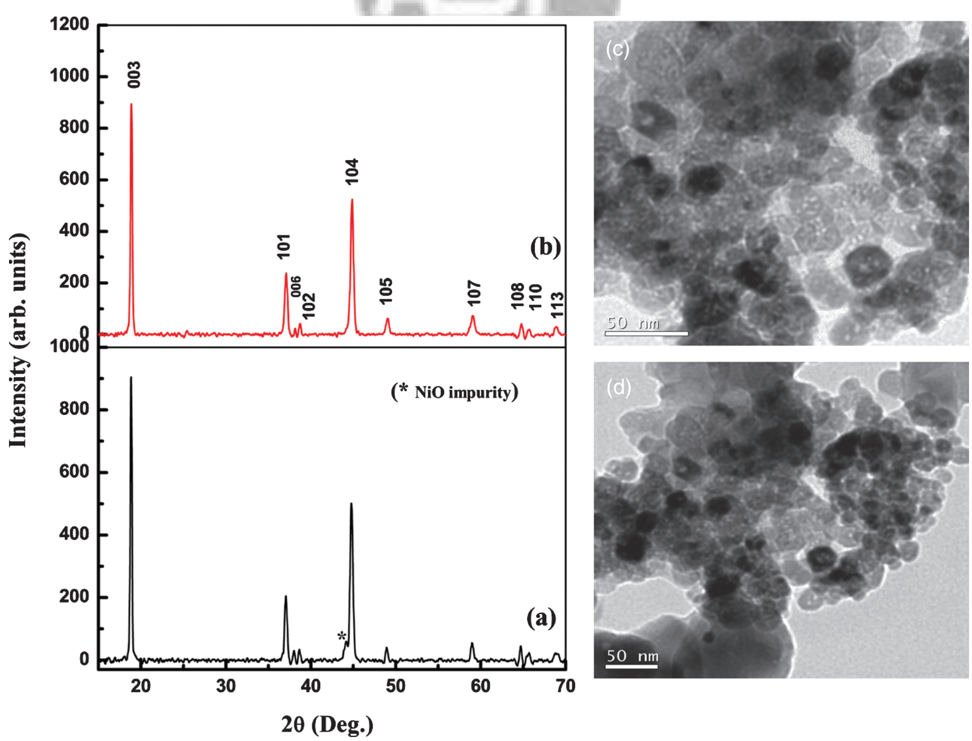

Fig. 2. (a) X-ray diffraction patterns of $LiCo_{1/3}Ni_{1/3}Mn_{1/3}O_2$ synthesized using a lithium: transition metal ratio of (a) 1:1 and (b) 1.1:1 [where transition metals are Co, Ni and Mn] and (c) and (d) TEM images captured for $LiCo_{1/3}Ni_{1/3}Mn_{1/3}O_2$ synthesized using a lithium: transition metal ratio of 1.1:1.

UK) X-ray photoelectron spectroscopy (XPS) using an Mg Kα (1253.6 eV) radiation. Electrochemical cycling and impedance behaviour were investigated using an Auto lab electrochemical workstation and the charge discharge studies were carried out using ORBIN charge-discharge cycle life tester.

2.3. Electrode Preparation and Cell Assembly

Details pertaining to electrode fabrication and 2032 coin cell assembly are reported elsewhere.[7] Electrochemical characterizations were carried out on freshly fabricated 2032 coin cells consisting of lithium anode, synthesized $LiCo_{1/3}Ni_{1/3}Mn_{1/3}O_2$ cathode and a non-aqueous electrolyte containing 1 M $LiPF_6$ dissolved in 1:1 v/v EC:PC with a cell guard separator.

3. RESULTS AND DISCUSSION

3.1. Phase and Surface Analysis

Figures 2(a)–(b) shows XRD patterns of the $LiCo_{1/3}Ni_{1/3}Mn_{1/3}O_2$ synthesized using a lithium and transition metal ratio of 1:1 and 1.1:1 individually. The recorded Bragg patterns can be indexed on α-$NaFeO_2$ type of layered structure with R-3m space group. It is evident from Figure 2(a) that a combination of stoichiometric ratio of lithium and transition metal (1:1) leads to the co-existence of impure and cubic NiO phase at $2\theta = 44°$, which in turn is reported to be an obstacle for the Li^+ ion movement due to its incompatibility with layered structure.[9] On the other hand, when a lithium and transition metal ratio of 1.1:1 was used, the extra lithium reacts with impure NiO phase and leads to phase pure and layered $LiCo_{1/3}Ni_{1/3}Mn_{1/3}O_2$, which is obvious from Figure 2(b). Further, the slightly decreased lattice parameter value ($a = 2.8511$ Å and $c = 14.1902$ Å) that results from the increased lithium content of starting materials is in agreement with the reported results.[9] Hence, $LiCo_{1/3}Ni_{1/3}Mn_{1/3}O_2$ synthesized from an optimized lithium: transition ratio of 1.1:1 (Fig 2(b)) alone is considered for further characterization.

Figure 2(b) shows the presence of distinct splitting of doublet at $2\theta = 38.5°$ and 65°, which is in favour of the perfect layered structure. In addition, the integrated intensity ratio $I_{(003)}/I_{(104)}$ value (1.71) of $LiCo_{1/3}Ni_{1/3}Mn_{1/3}O_2$

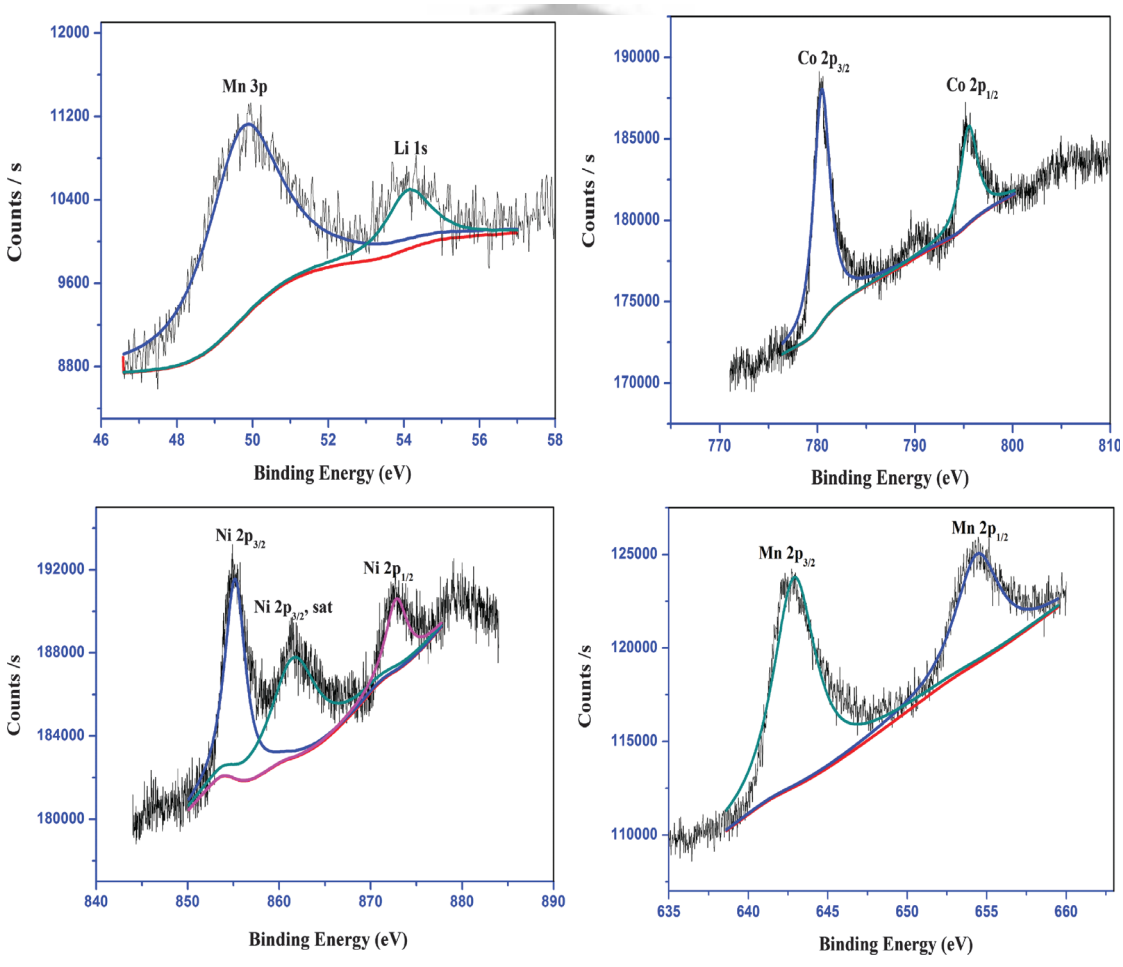

Fig. 3. XPS spectra of $LiCo_{1/3}Ni_{1/3}Mn_{1/3}O_2$ compound.

compound indicates good cation ordering,[10] which is quite encouraging.

The nanocrystalline nature and the presence of 50 nm particles of $LiCo_{1/3}Ni_{1/3}Mn_{1/3}O_2$ material prepared by sol–gel method with 1.1:1 of Li:M has been evidenced by transmission electron microscopy (Fig. 2(b)). Presence of homogeneous distribution of nano sized particles with definite grain boundary in the order of 50 nm is seen from the TEM image. Hence, it is understood that the currently adopted modified sol–gel method is effective in significantly reducing the particle size, which is desirable for the facile lithium intercalation behaviour of cathode materials.

3.2. X-Ray Photoelectron Spectroscopy Study

The oxidation state of the individual metal atoms present in $LiCo_{1/3}Ni_{1/3}Mn_{1/3}O_2$ compound is confirmed from XPS analysis. Figure 3 shows the binding energy values of Li 1s, Ni $2p_{3/2}$, Co $2p_{3/2}$ and Mn $2p_{3/2}$ of $LiCo_{1/3}Ni_{1/3}Mn_{1/3}O_2$ compound respectively. In the Ni XPS spectrum (Fig. 3(b)), a characteristic satellite peak is noted in addition to the Ni ($2p_{3/2}$) peak. Such a satellite peak due to the multielectron excitation (shake up peaks) is usually observed with $Ni(OH)_2$.[11, 12] Further, curve fitting of the Ni $2p_{3/2}$ signals at 855 eV also agrees with that reported for $Ni(OH)_2$,[11, 12] thus confirming the oxidation state of Ni as +2. The best fit for the Co $2p_{3/2}$spectrum (Fig. 3(c)) corresponding to a Co^{3+} binding energy value of 780.57 eV agrees well with the reported Co^{3+} value of Shaju et al.[13] Similarly, the Mn XPS spectrum (Fig. 3(d)) has a major peak located at a binding energy of 642.2 eV, corresponding to the reported values of Mn^{4+}state.[5] Based on these results, the oxidation state of Ni, Co and Mn ions of currently synthesized $LiCo_{1/3}Ni_{1/3}Mn_{1/3}O_2$ compound is confirmed as 2^+, 3^+ and 4^+ respectively and the average transition metal valency of 3^+ is thus validated.

3.3. Electrochemical Characterizations

Cyclic voltammograms of $LiCo_{1/3}Ni_{1/3}Mn_{1/3}O_2$ cathode were recorded at different scan rates such as 0.1, 0.2, 0.3, 0.4 and 0.5 mV/sec. (Fig. 4(a)), with a view to understand the effect and extent of individual transtion metals in imparting specific capacity as a function of varying scan rates. The CV recorded at 0.1 mV/sec. consists of a red-ox couple at 3.95 and 3.77 V corresponding to Ni^{2+}/Ni^{4+} pair and another at 4.53 and 4.42 V, corresponding to Co^{3+}/Co^{4+} pair.[5] Mn^{4+}, being an electrochemically inactive species gives rise to no

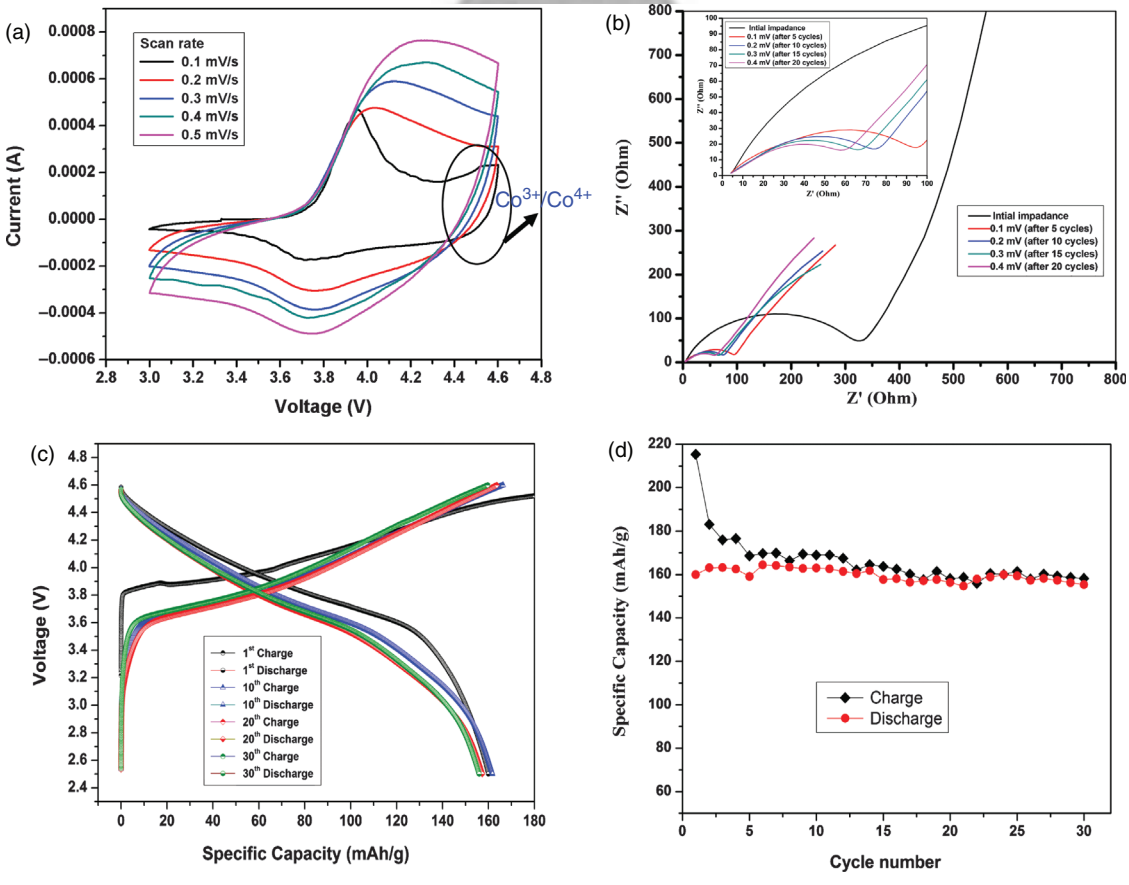

Fig. 4. (a) Cyclic Voltammograms and (b) Nyquist impedance behaviour of $LiCo_{1/3}Ni_{1/3}Mn_{1/3}O_2$ cathode at different scan rates (c) Voltage versus capacity behaviour of $LiCo_{1/3}Ni_{1/3}Mn_{1/3}O_2$ cathode and (d) Cycleability of $LiCo_{1/3}Ni_{1/3}Mn_{1/3}O_2$ cathode synthesized using modified sol–gel method.

CV signal, which is justifiable. Hence, the facile intercalation and de-intercalation behaviour of Li^+ ions in $LiCo_{1/3}Ni_{1/3}Mn_{1/3}O_2$ cathode and the respective oxidation states of Ni^{+2}, Co^{+3} and Mn^{+4}, as derived from XPS studies are confirmed further from CV studies. Further, it is evident from Figure 4(a) that with the increasing scan rate, cobalt red-ox pair (Co^{3+}/Co^{4+}) is found to dissapear and the anodic peaks of Ni^{2+}/Ni^{4+} are correspondingly broadened and shifted towards slightly higher voltage regions, without altering the position of broadened cathodic peaks. Hereagain, the appearance of comparatively reduced cathodic peak is not unusal, as literature is replete with evidences on similar kind of broadening and reduced cathodic peak current behavior of the title compound.[14, 15] While the varying anodic and cathodic peak currents could be understood as a function of linear relationship of CV peak currents with the square root of scan rates,[16] the disapperance of Co^{3+}/Co^{4+} peak pair at higher scan rates evidences the fact that Ni^{2+}/Ni^{4+} peak pair is the major contributing redox pair, as far as the capacity behavior of $LiCo_{1/3}Ni_{1/3}Mn_{1/3}O_2$ is concerned.

The structural stability of $LiCo_{1/3}Ni_{1/3}Mn_{1/3}O_2$ cathode is understood from Figure 4(b) that corresponds to the electrochemical impedance behavior of the same as a function of different scan rates such as 0.1, 0.2, 0.3 and 0.4 mV/sec. Interestingly, the R_{ct} value of the as fabricated Li/$LiCo_{1/3}Ni_{1/3}Mn_{1/3}O_2$ cell is found to decrease from 320 Ω to 95 Ω under the influence of 0.1 mV/sec. scan rate, which is in favor of the stabilization of electrode-electrolyte interface. As the scan rate increses, the R_{ct} value reduces further that corresponds to a high rate of electron transfer between the electrode and electrolyte interface. Even after an increased scan rate of 0.4 mV/sec., a smaller impedance value of 65 Ω is observed along with the retention of shape of the semicircle (Fig. 4(b)) and hence the structural stability of $LiCo_{1/3}Ni_{1/3}Mn_{1/3}O_2$ cathode at different current densities is understood.

The specific capacity versus volatge behavior and the cycleability of $LiCo_{1/3}Ni_{1/3}Mn_{1/3}O_2$ cathode synthesized using modified sol–gel method at 0.1 C rate are described in Figures 4(c) and (d). Duly stabilized electrode-electrolyte interface driven steady-state charge-discharge capacity behavior with a columbic efficiency of 99% is observed, especially after 5 cycles (Figs. 4(c and d)). Interestingly, $LiCo_{1/3}Ni_{1/3}Mn_{1/3}O_2$ cathode delivered a steady state capacity as high as 162 mAh/g with an excellent capacity retention and a negligible capacity fade (1%) up to 30 cycles (Fig. 4(d)). Hence, the negligible capacity fade behavior, as expected from the smaller impedance values is substantiated from the charge-discharge behavior of $LiCo_{1/3}Ni_{1/3}Mn_{1/3}O_2$ cathode. Such an improved electrochemical behavior of $LiCo_{1/3}Ni_{1/3}Mn_{1/3}O_2$ cathode has been endorsed to the synergistic effect of nano sized particles (~50 nm) derived from modified sol–gel method and the phase purity of the title compound achieved by choosing a Li:M ratio of 1.1:1 in the precursor mix.

4. CONCLUSION

Layered $LiCo_{1/3}Ni_{1/3}Mn_{1/3}O_2$ cathode material has been synthesized in the form of phase pure and nanocrystalline powder by adopting modified sol–gel method. Significantly reduced gel formation time and enhanced phase purity are achieved by using ammonium per sulphate as gelling agent and a Li:M ratio of 1.1:1 respectively. XRD and TEM results confirm the formation of phase pure compound with a particle size of 50 nm. Oxidation state of metal species in the sol–gel synthesized $LiCo_{1/3}Ni_{1/3}Mn_{1/3}O_2$ compound is confirmed as Ni^{2+}, Co^{3+} and Mn^{4+} using XPS analysis. The exceeding role of Ni^{2+}/Ni^{4+} peak pairs in exhibiting steady-state capacity behaviour and the structural stability of $LiCo_{1/3}Ni_{1/3}Mn_{1/3}O_2$ cathode are demonstrated from CV and impedance studies. Further, charge-discharge study evidences a high discharge capacity (162 mAh/g) with an excellent capacity retention (99%) upon extended cycling (30 cycles). The study recommends that the currently adopted modified sol–gel method is yet another potential approach to synthesize nanocrystalline $LiCo_{1/3}Ni_{1/3}Mn_{1/3}O_2$ compound, suitable for rechargeable lithium battery applications.

Acknowledgments: The authors are thankful to the Council of Scientific and Industrial Research (CSIR), India for financial support to carry out this work through Inter Agency Project (IAP-04). Dr. T. Premkumar is gratefully acknowledged for extending the charge-discharge cycling facilities.

References and Notes

1. S. T. Myung, S. Komabo, N. Hirosaki, H. Yashiro, and N. Kumagai, *Electrochim. Acta* 49, 4213 (**2004**).
2. Y. Idemoto and T. Matsui, *Solid State Ionics* 179, 625 (**2008**).
3. N. Yabuuchi and T. Ohzuku, *J. Power Sources* 171, 119 (**2003**).
4. J. Guo, L. F. Jiao, H. T. Yuan, H. X. Li, M. Zhang, and Y. M. Wang, *Electrochim. Acta* 51, 3731 (**2006**).
5. K. M. Shaju, G. V. Subba Rao, and B. V. R. Chowdari, *Electrochim. Acta* 48, 145 (**2002**).
6. T. H. Cho, S. M. Park, M. Yoshia, T. Hirai, and Y. Hideshima, *J. Power Sources* 142, 306 (**2005**).
7. Gangulibabu, D. Bhuvaneswari, N. Kalaiselvi, N. Jayaprakash, and P. Periasamy, *J. Sol–Gel Sci. Technol.* 49, 137 (**2009**).
8. M. Balandeh and S. Asgari, *J. Nano Materials* 2010, 695083 (**2010**).
9. L. Zhang, X. Wang, T. Muta, D. Li, H. Noguchi, M. Yoshio, R. Ma, and T. Takada, *J. Power Sources* 162, 629 (**2006**).
10. P. Reale, D. Privitera, S. Panero, and B. Scrosati, *Solid State Ionics* 178, 1390 (**2007**).

11. G. Casella, M. R. Guascito, and M. G. Sannazzaro, *J. Electroanal. Chem.* 462, 202 **(1999)**.
12. Y. Zhao, Y. E. L. Fan, Y. Qiu, and S. Yang, *Electrochim. Acta* 52, 5873 **(2007)**.
13. K. M. Shaju, G. V. Subba Rao, and B. V. R. Chowdari, *Solid State Ionics* 69, 152 **(2002)**.
14. G. T. K. Fey, C. S. Chang, and T. Prem Kumar, *J. Solid State Electrochem.* 14, 17 **(2010)**.
15. F. Wu, M. Wang, Y. Su, and S. Chen, *J. Power Sources* 189, 743 **(2009)**.
16. C. Y. Yao, T. H. Kao, C. H. Cheng, J. M. Chen, and W. H. Hurng, *J. Power Sources* 54, 491 **(1995)**.

Received: 12 October 2010. Accepted: 14 February 2011.